

Figure 2.1 Three types of potentiometric devices for measuring displacements (a) Translational. (b) Single-turn. (c) Multi-turn. (From *Measurement Systems: Application and Design*, by E. O. Doebelin. Copyright © 1990 by McGraw-Hill, Inc. Used with permission of McGraw-Hill Book Co.)

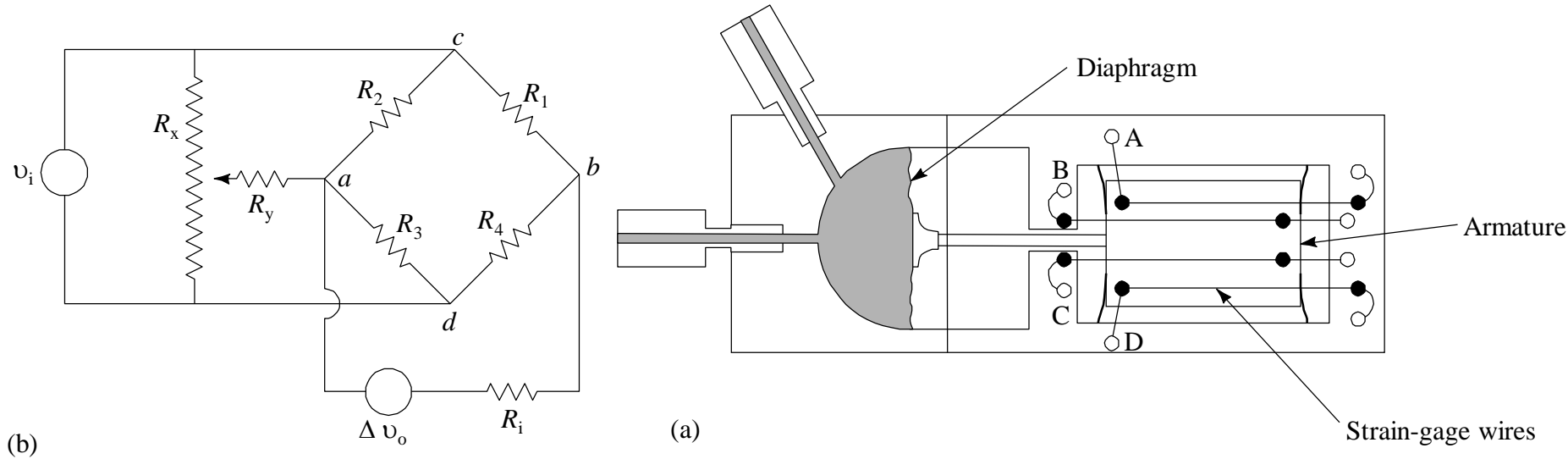


Figure 2.2 (a) Unbonded strain-gage pressure sensor. The diaphragm is directly coupled by an armature to an unbonded strain-gage system. With increasing pressure, the strain on gage pair B and C is increased, while that on gage pair A and D is decreased. (b) Wheatstone bridge with four active elements. $R_1 = A$, $R_2 = B$, $R_3 = D$, and $R_4 = C$ when the unbonded strain gage is connected for translation motion. Resistor R_y and potentiometer R_x are used to initially balance the bridge. v_i is the applied voltage and Δv_o is the output voltage on a voltmeter or similar device with an internal resistance of R_i .

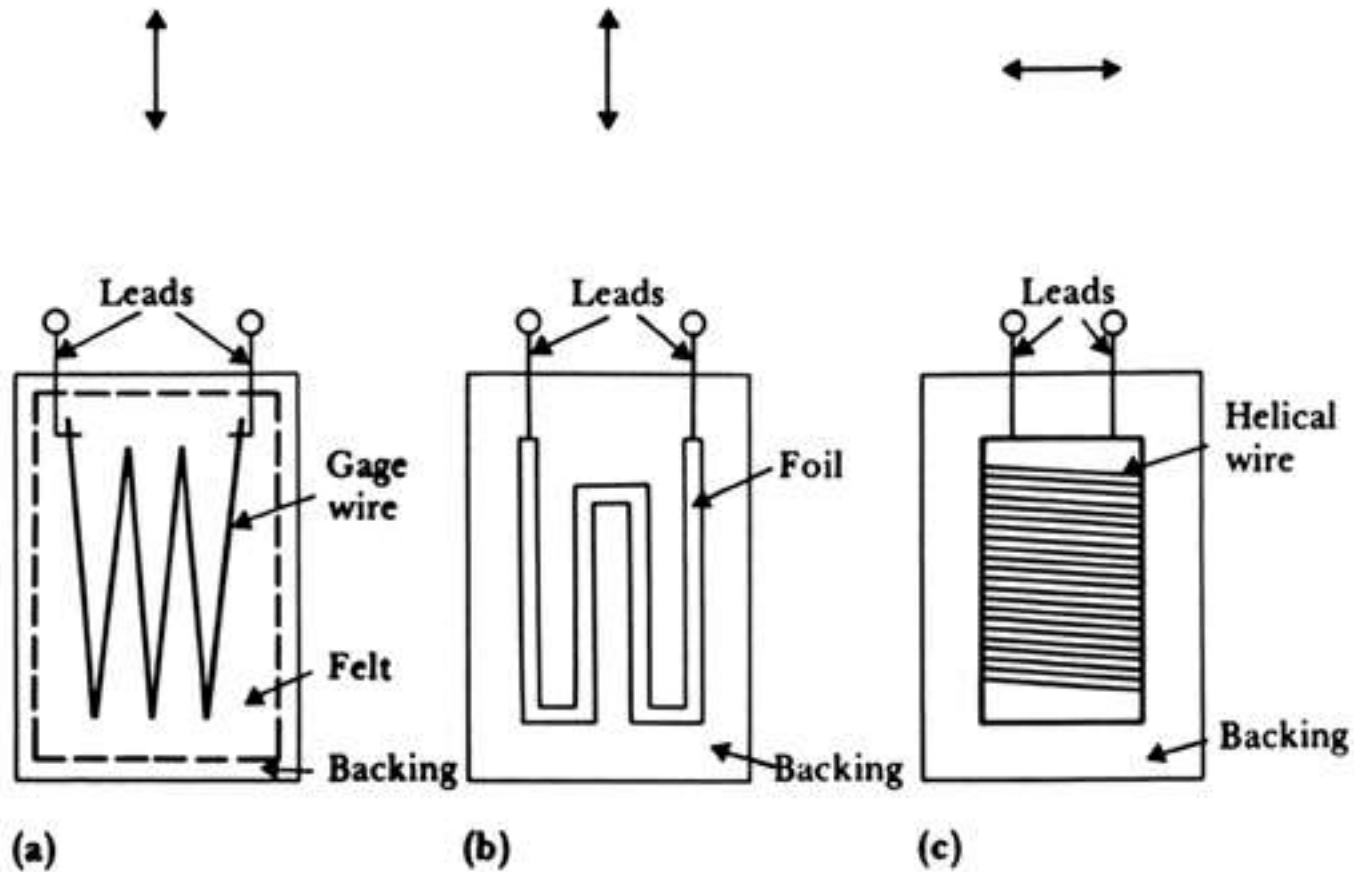
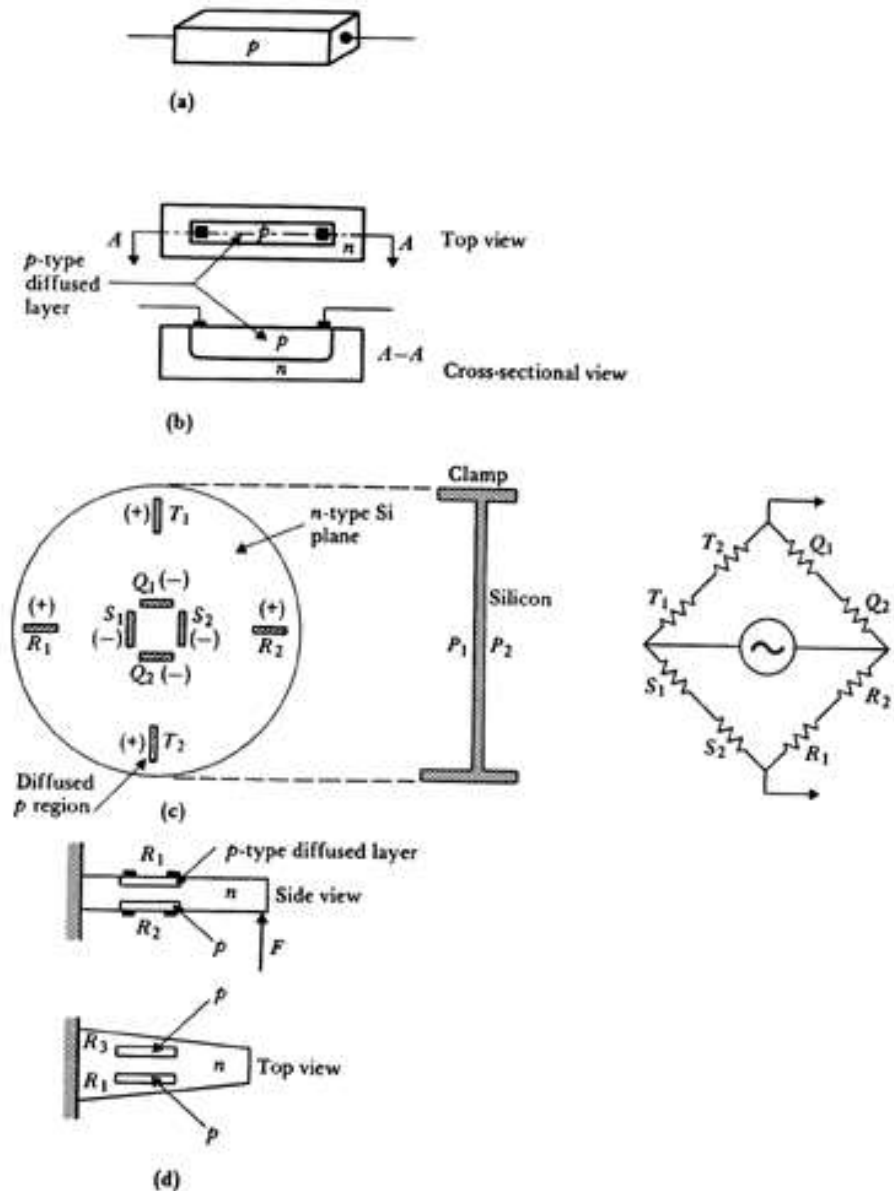


Figure 2.3 Typical bonded strain-gage units (a) Resistance-wire type. (b) Foil type. (c) Helical-wire type. Arrows above units show direction of maximal sensitivity to strain.[Parts (a) and (b) are modified from *Instrumentation in Scientific Research*, by K. S. Lion. Copyright © 1959 by McGraw-Hill, Inc. Used with permission of McGraw-Hill Book Co.]

Figure 2.4 Typical semiconductor strain-gage units (a) Unbonded, uniformly doped. (b) Diffused p-type gage. (c) Integrated pressure sensor. (d) Integrated cantilever-beam force sensor. (From Transducers for Biomedical Measurements: Application and Design, by R. S. C. Cobbold. Copyright © 1974, John Wiley and Sons, Inc. Used by permission of John Wiley and Sons, Inc.)



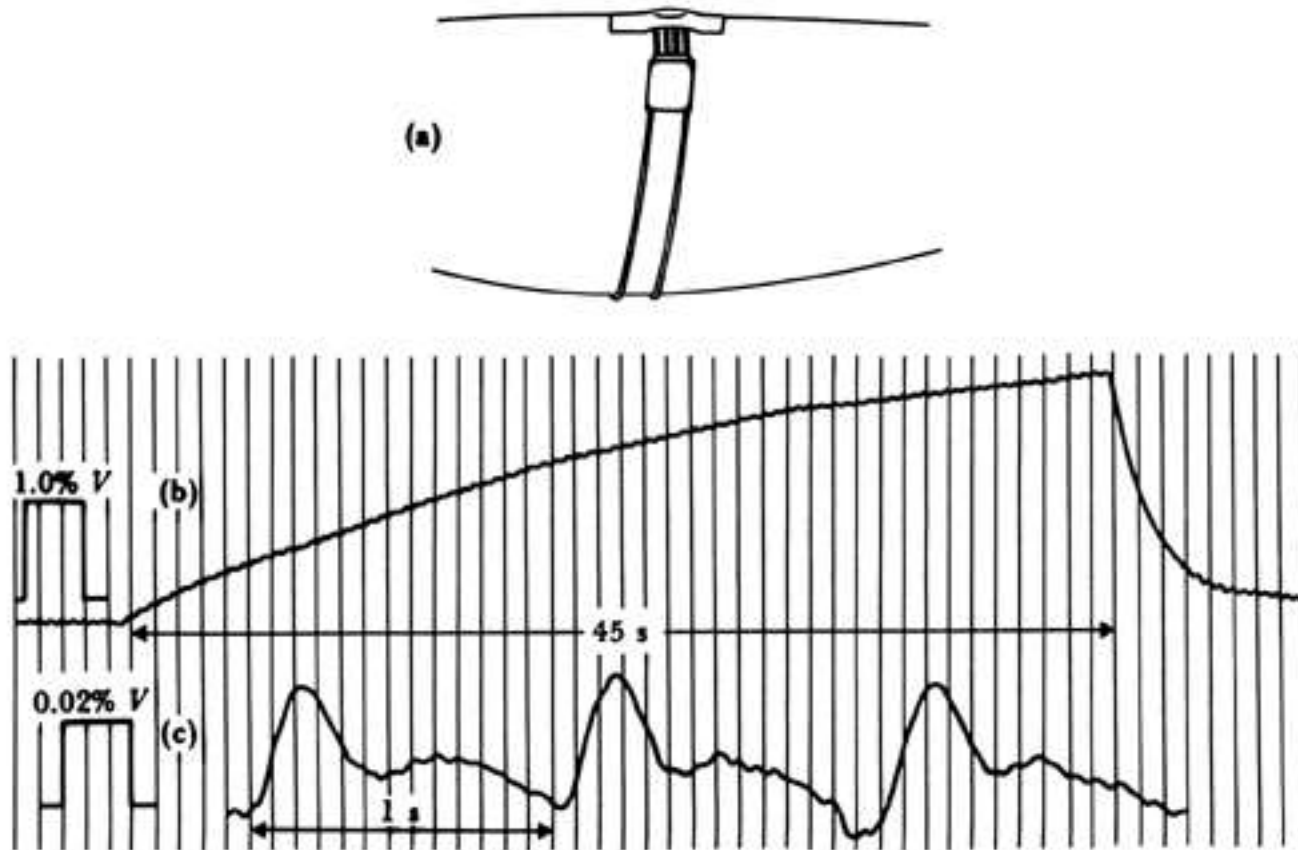


Figure 2.5 Mercury-in-rubber strain-gage plethysmography (a) Four-lead gage applied to human calf. (b) Bridge output for venous-occlusion plethysmography. (c) Bridge output for arterial-pulse plethysmography. [Part (a) is based on D. E. Hokanson, D. S. Sumner, and D. E. Strandness, Jr., "An electrically calibrated plethysmograph for direct measurement of limb blood flow." 1975, BME-22, 25-29; used with permission of IEEE Trans. Biomed. Eng., 1975, New York.]

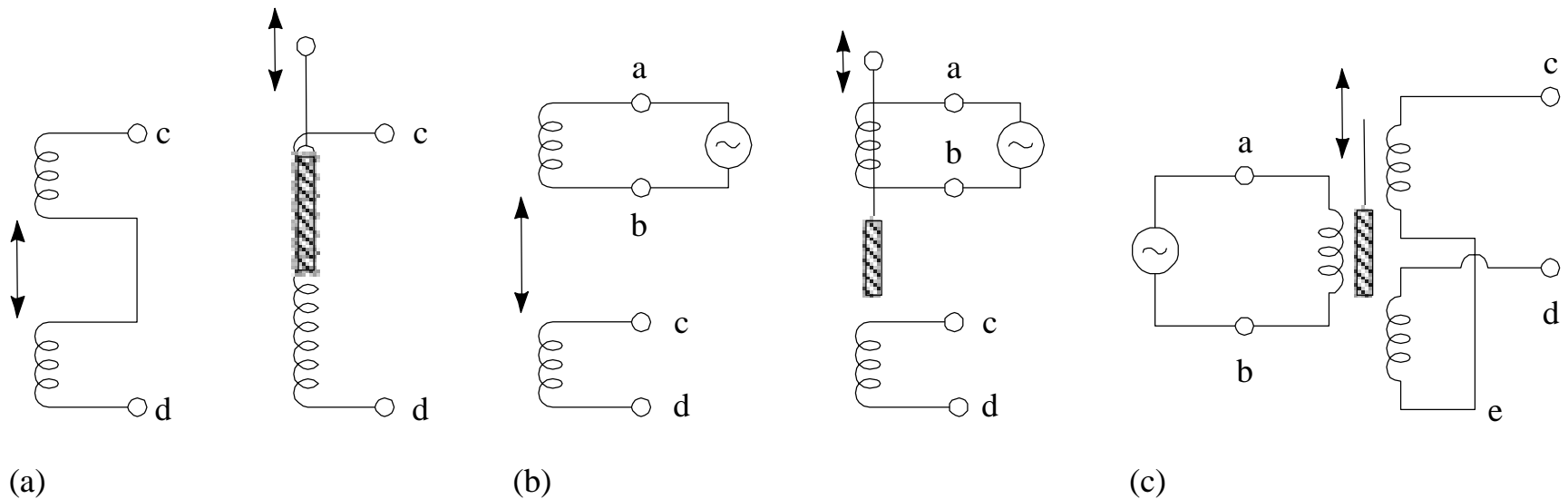
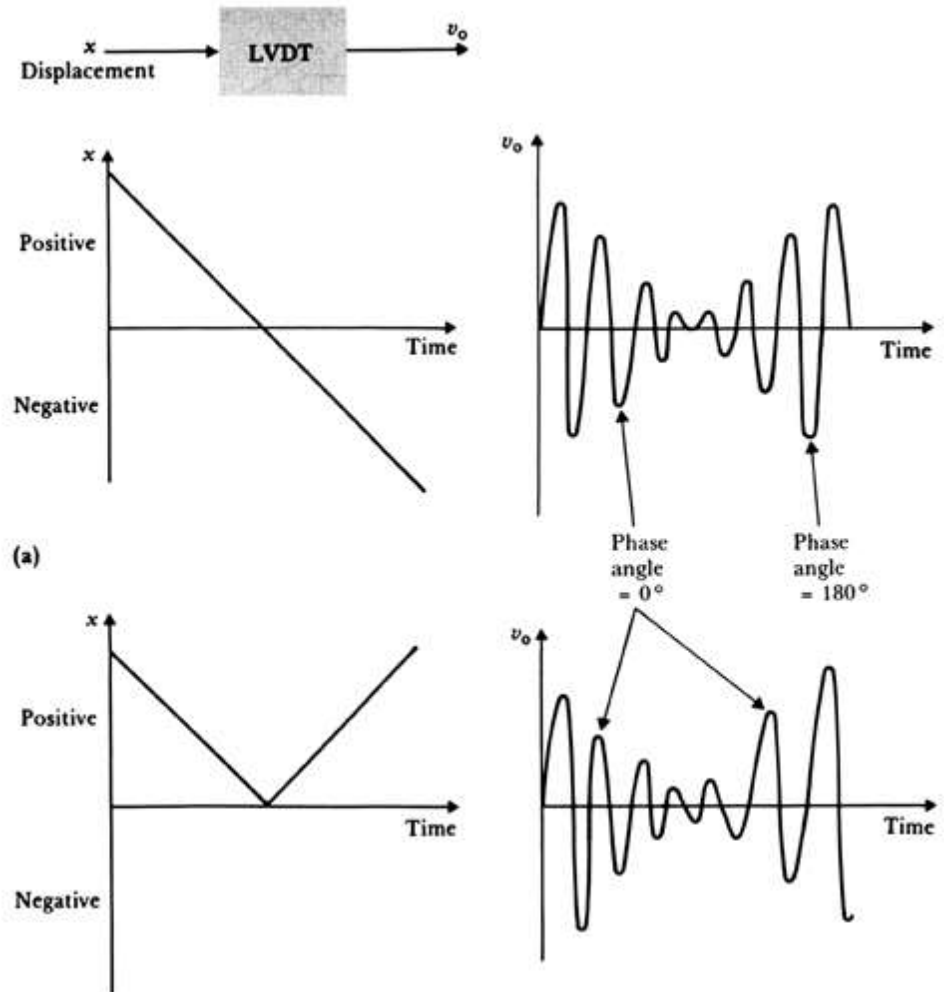


Figure 2.6 Inductive displacement sensors (a) Self-inductance. (b) Mutual inductance. (c) Differential transformer.

Figure 2.7 (a) As x moves through the null position, the phase changes 180° , while the magnitude of v_o is proportional to the magnitude of x . (b) An ordinary rectifier-demodulator cannot distinguish between (a) and (b), so a phase-sensitive demodulator is required.



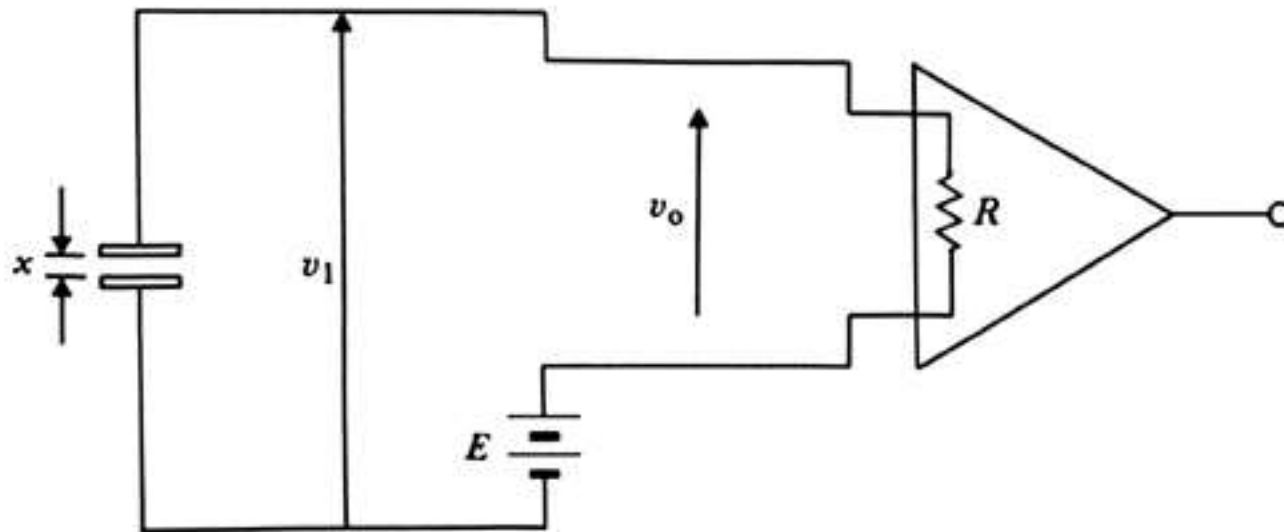


Figure 2.8 Capacitance sensor for measuring dynamic displacement changes

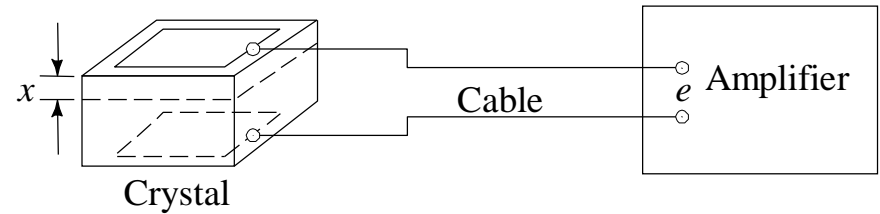
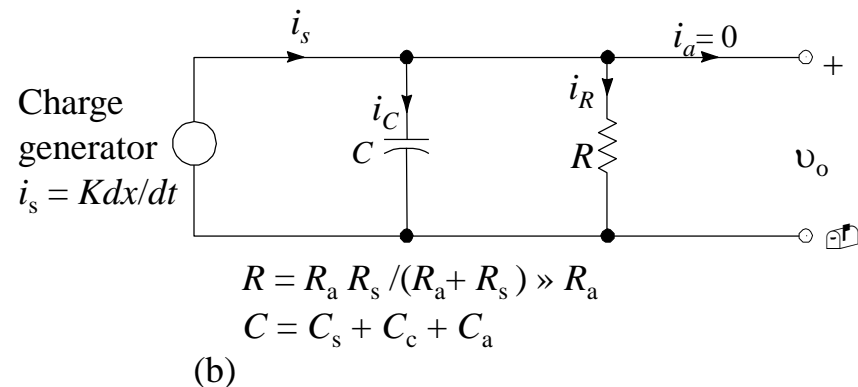
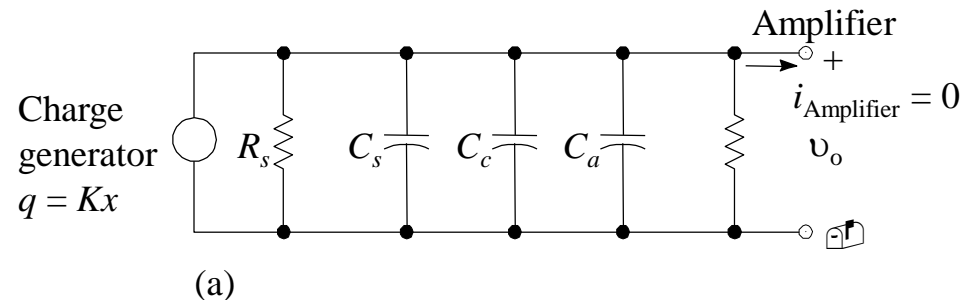


Figure 2.9 (a) Equivalent circuit of piezoelectric sensor, where R_s = sensor leakage resistance, C_s = sensor capacitance, C_c = cable capacitance, C_a = amplifier input capacitance, R_a = amplifier input resistance, and q = charge generator. (b) Modified equivalent circuit with current generator replacing charge generator. (From Measurement Systems: Application and Design, by E. O. Doebelin. Copyright © 1990 by McGraw-Hill, Inc. Used with permission of McGraw-Hill Book Co.)



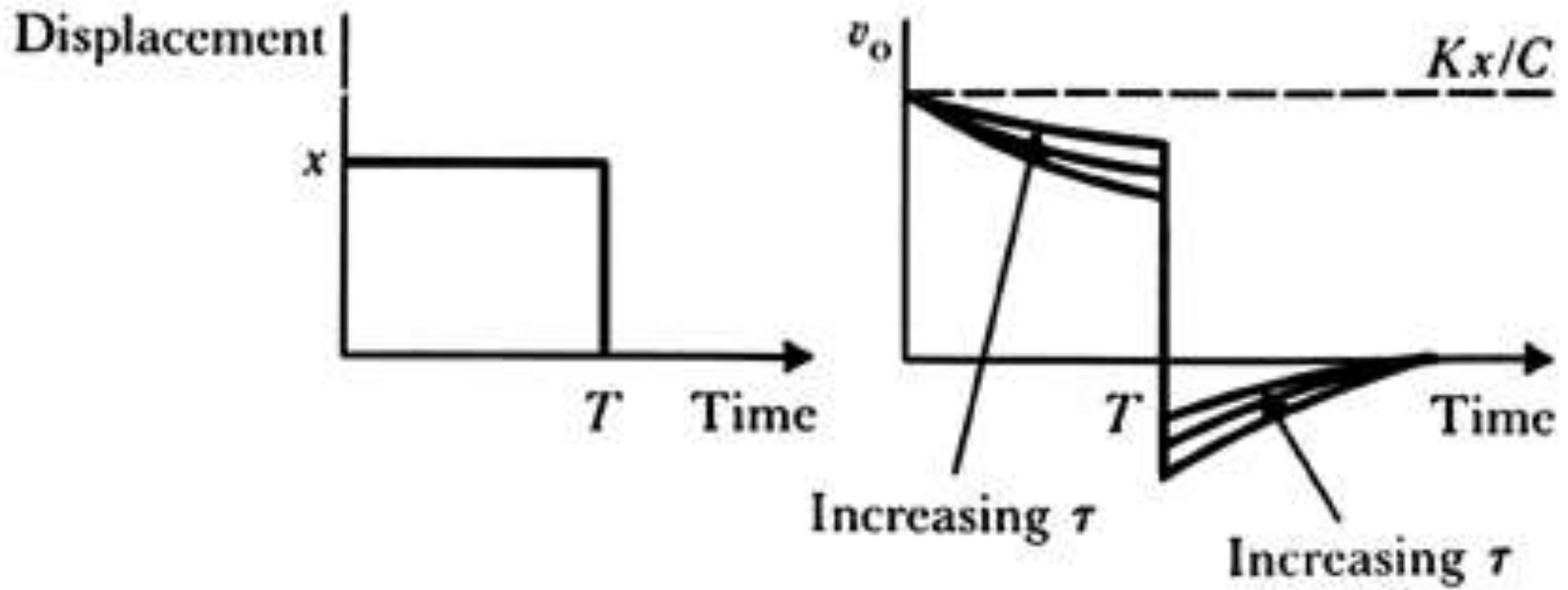


Figure 2.10 Sensor response to a step displacement (From Measurement Systems: Application and Design, by E. O. Doebelin. Copyright © 1990 by McGraw-Hill, Inc. Used with permission of McGraw-Hill Book Co.)

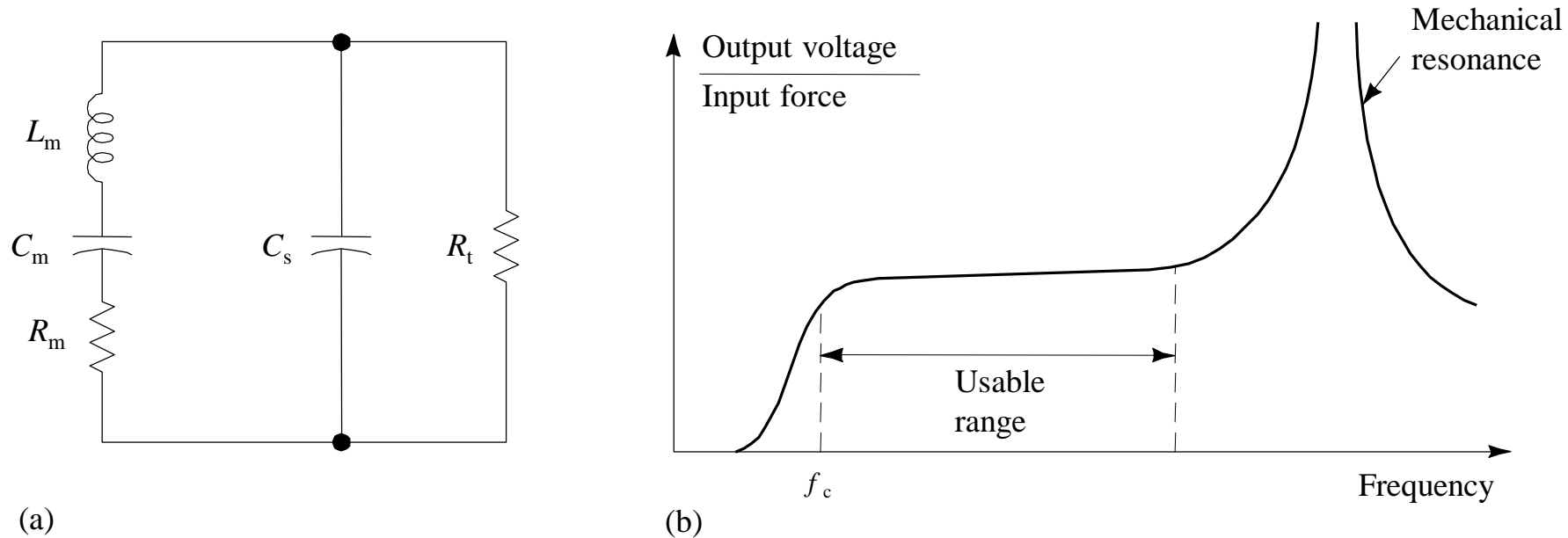


Figure 2.11 (a) High-frequency circuit model for piezoelectric sensor. R_s is the sensor leakage resistance and C_s the capacitance. L_m , C_m , and R_m represent the mechanical system. (b) Piezoelectric sensor frequency response. (From *Transducers for Biomedical Measurements: Application and Design*, by R. S. C. Cobbold. Copyright © 1974, John Wiley and Sons, Inc. Used by permission of John Wiley and Sons, Inc.)

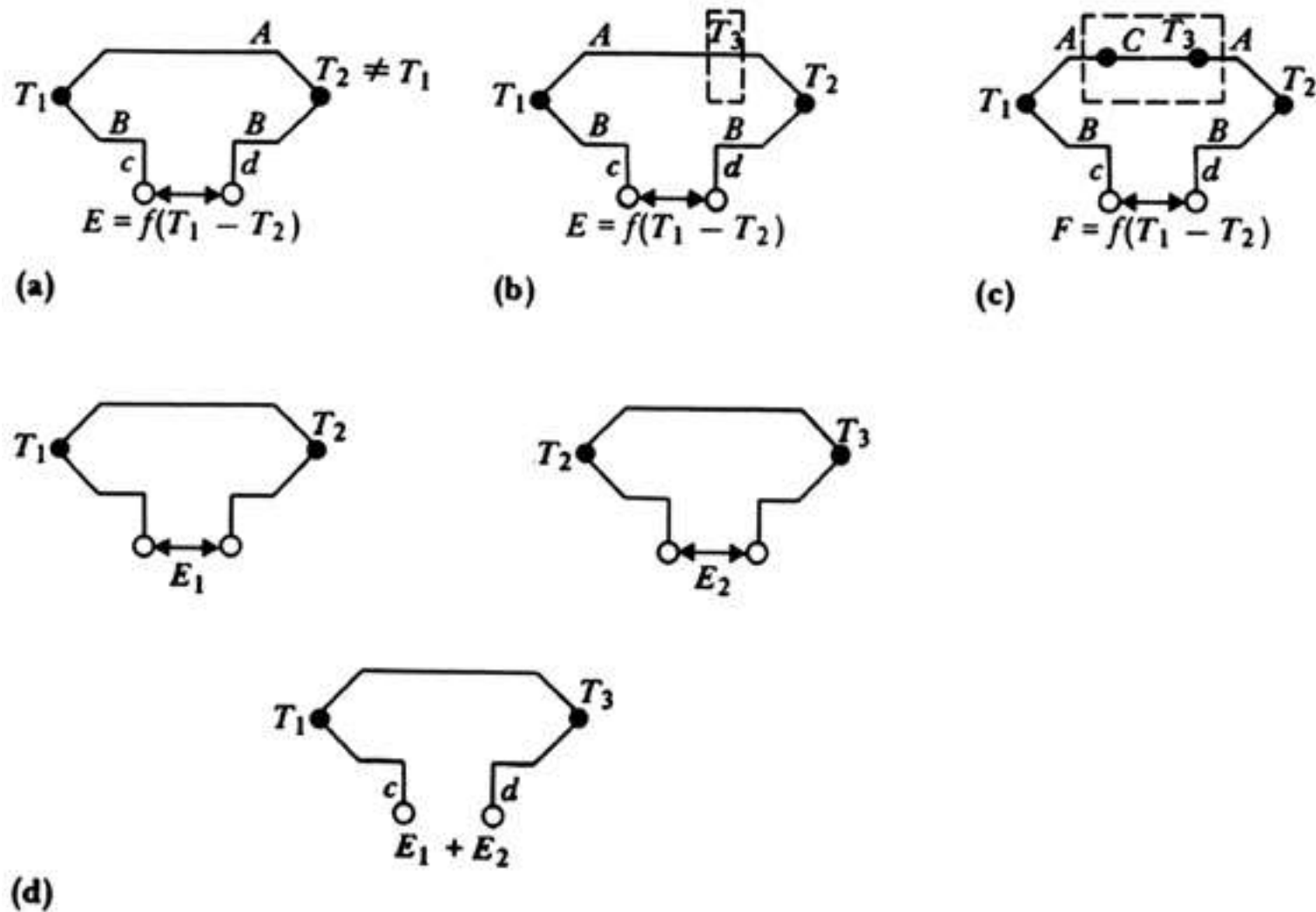
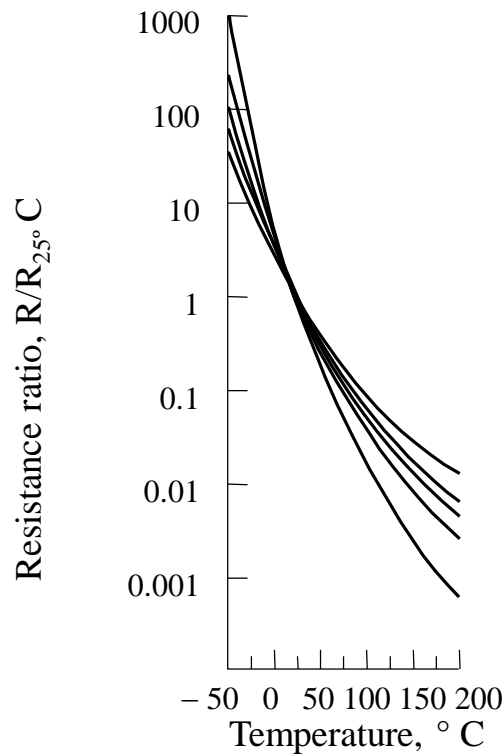
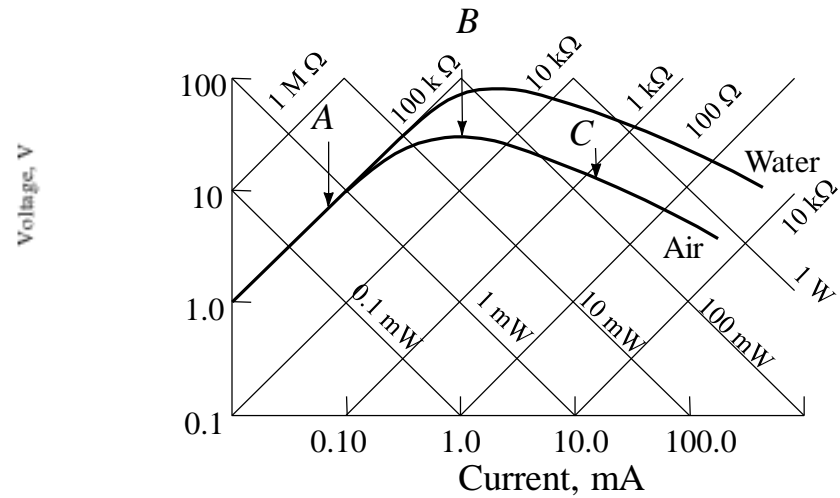


Figure 2.12 Thermocouple circuits (a) Peltier emf. (b) Law of homogeneous circuits. (c) Law of intermediate metals. (d) Law of intermediate temperatures.



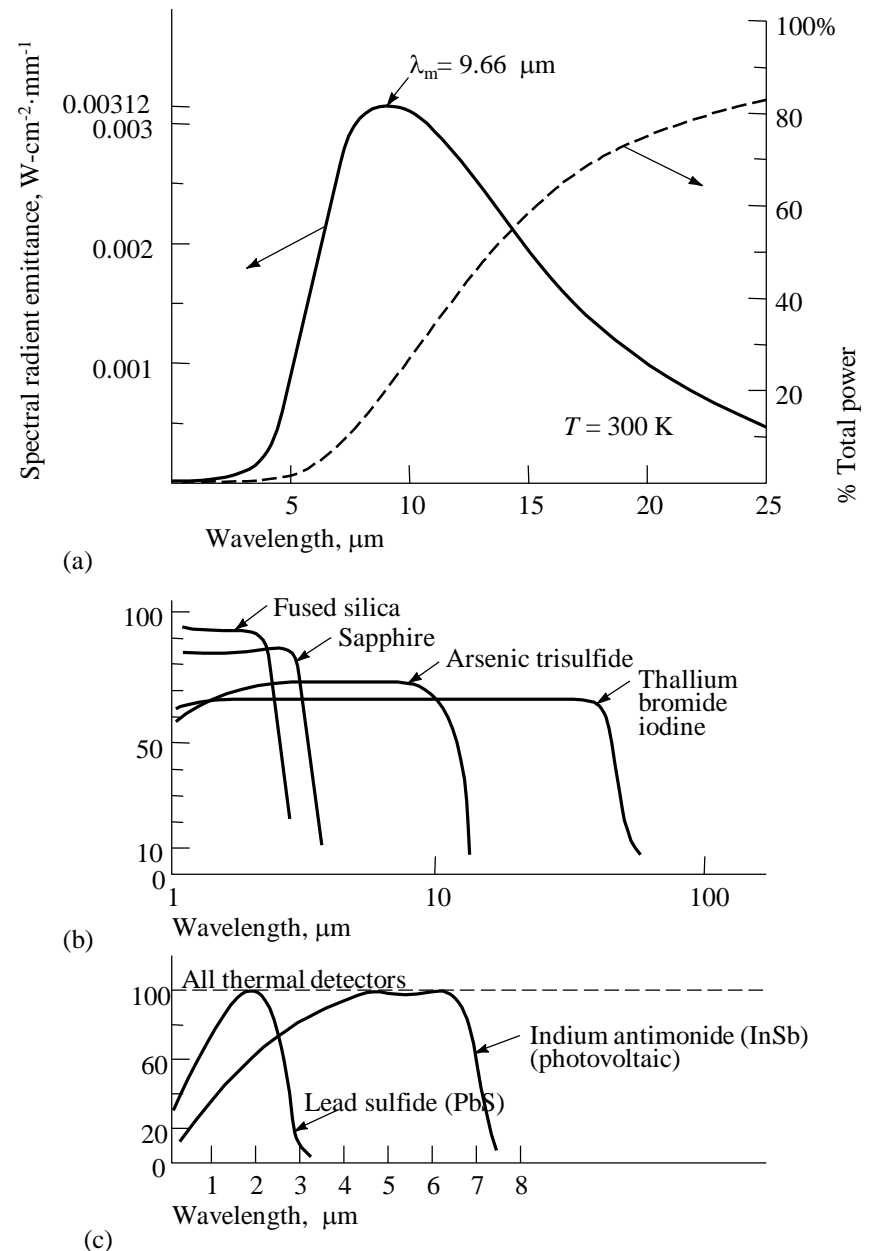
(a)



(b)

Figure 2.13 (a) Typical thermistor zero-power resistance ratio-temperature characteristics for various materials. (b) Thermistor voltage-versus-current characteristic for a thermistor in air and water. The diagonal lines with a positive slope give linear resistance values and show the degree of thermistor linearity at low currents. The intersection of the thermistor curves and the diagonal lines with the negative slope give the device power dissipation. Point A is the maximal current value for no appreciable self-heat. Point B is the peak voltage. Point C is the maximal safe continuous current in air. [Part (b) is from Thermistor Manual, EMC-6, © 1974, Fenwal Electronics, Framingham, MA; used by permission.]

Figure 2.14 (a) Spectral radiant emittance versus wavelength for a blackbody at 300 K on the left vertical axis; percentage of total energy on the right vertical axis. (b) Spectral transmission for a number of optical materials. (c) Spectral sensitivity of photon and thermal detectors. [Part (a) is from *Transducers for Biomedical Measurements: Principles and Applications*, by R. S. C. Cobbold. Copyright © 1974, John Wiley and Sons, Inc. Reprinted by permission of John Wiley and Sons, Inc. Parts (b) and (c) are from *Measurement Systems: Application and Design*, by E. O. Doebelin. Copyright © 1990 by McGraw-Hill, Inc. Used with permission of McGraw-Hill Book Co.]



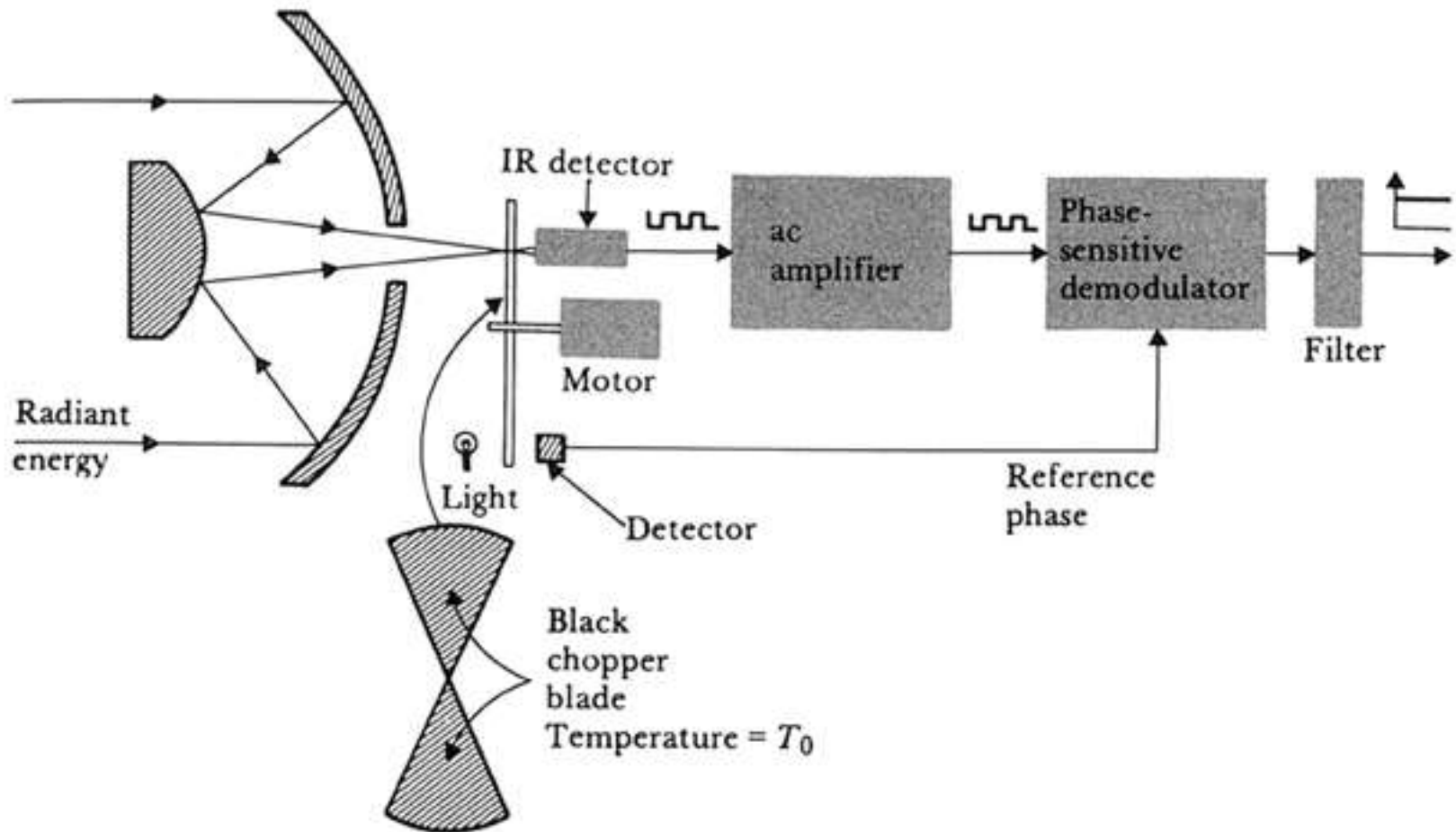


Figure 2.15 Stationary chopped-beam radiation thermometer (From Transducers for Biomedical Measurements: Principles and Applications, by R. S. C. Cobbold. Copyright © 1974, John Wiley and Sons, Inc. Reprinted by permission of John Wiley and sons. Inc.)

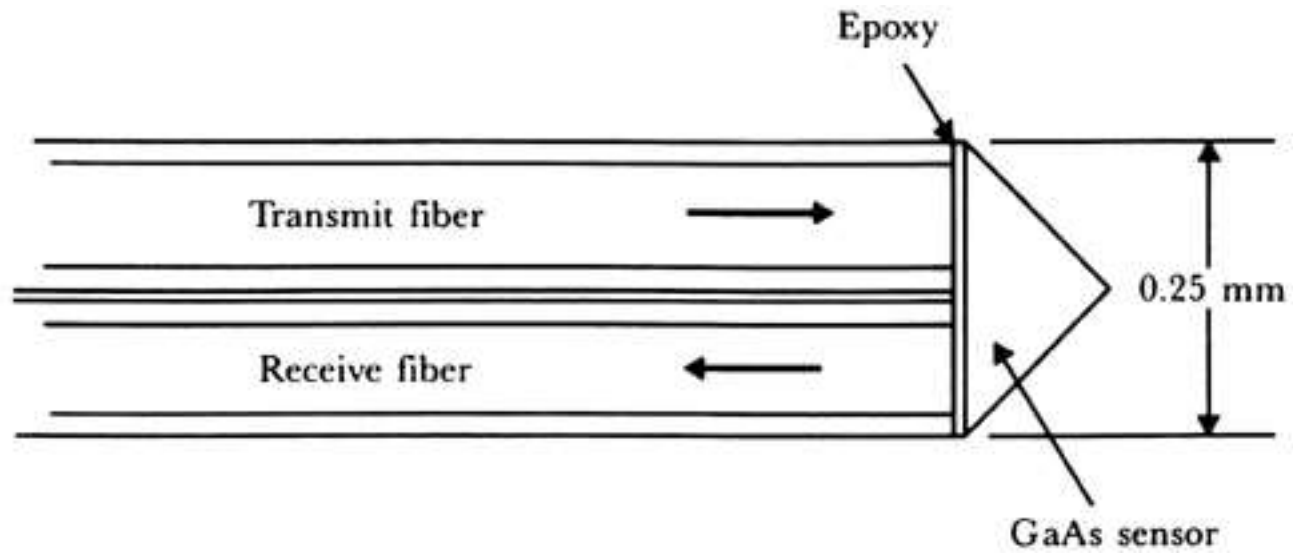
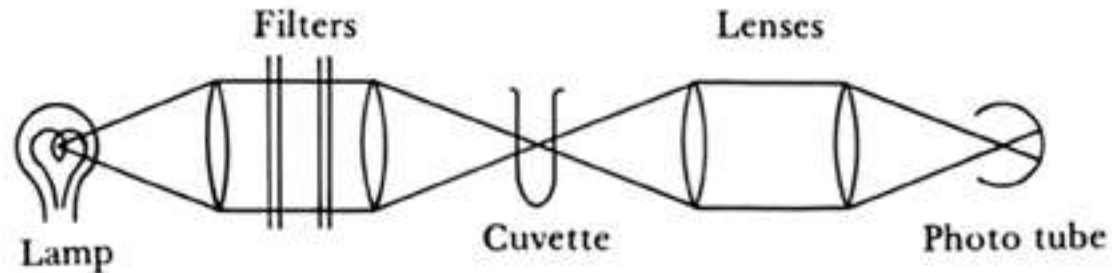


Figure 2.16 Details of the fiber/sensor arrangement for the GaAs semiconductor temperature probe.

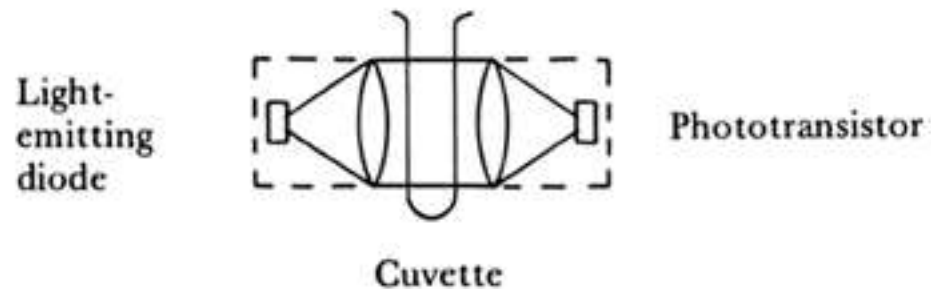


(a)

Figure 2.17 (a) General block diagram of an optical instrument. (b) Highest efficiency is obtained by using an intense lamp, lenses to gather and focus the light on the sample in the cuvette, and a sensitive detector. (c) Solid-state lamps and detectors may simplify the system.

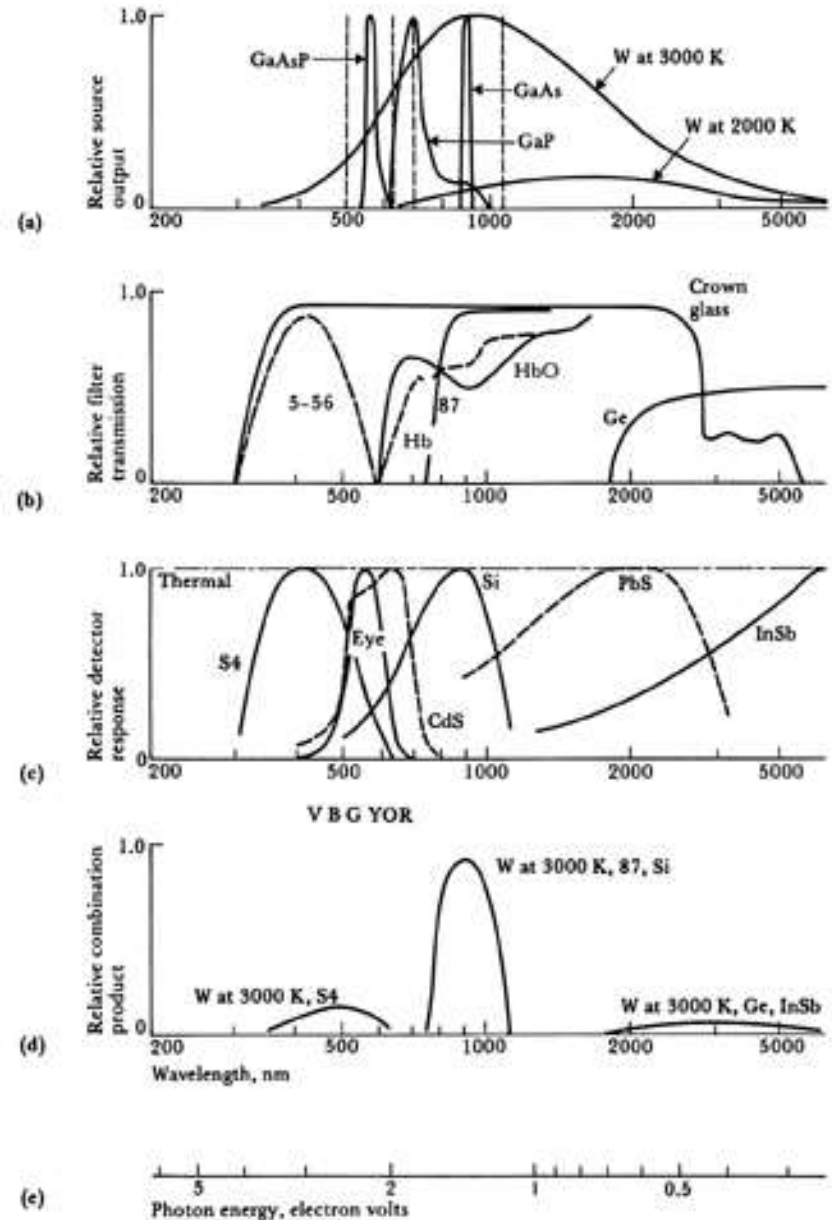


(b)



(c)

Figure 2.18 Spectral characteristics of sources, filters, detectors, and combinations thereof (a) Light sources, Tungsten (W) at 3000 K has a broad spectral output. At 2000 K, output is lower at all wavelengths and peak output shifts to longer wavelengths. Light-emitting diodes yield a narrow spectral output with GaAs in the infrared, GaP in the red, and GaAsP in the green. Monochromatic outputs from common lasers are shown by dashed lines: Ar, 515 nm; HeNe, 633 nm; ruby, 693 nm; Nd, 1064 nm; CO₂ (not shown), 10600 nm. (b) Filters. A Corning 5-65 glass filter passes a blue wavelength band. A Kodak 87 gelatin filter passes infrared and blocks visible wavelengths. Germanium lenses pass long wavelengths that cannot be passed by glass. Hemoglobin Hb and oxyhemoglobin HbO pass equally at 805 nm and have maximal difference at 660 nm. (c) Detectors. The S4 response is a typical phototube response. The eye has a relatively narrow response, with colors indicated by VBG YOR. CdS plus a filter has a response that closely matches that of the eye. Si p-n junctions are widely used. PbS is a sensitive infrared detector. InSb is useful in far infrared. Note: These are only relative responses. Peak responses of different detectors differ by 107. (d) Combination. Indicated curves from (a), (b), and (c) are multiplied at each wavelength to yield (d), which shows how well source, filter, and detector are matched. (e) Photon energy: If it is less than 1 eV, it is too weak to cause current flow in Si p-n junctions.



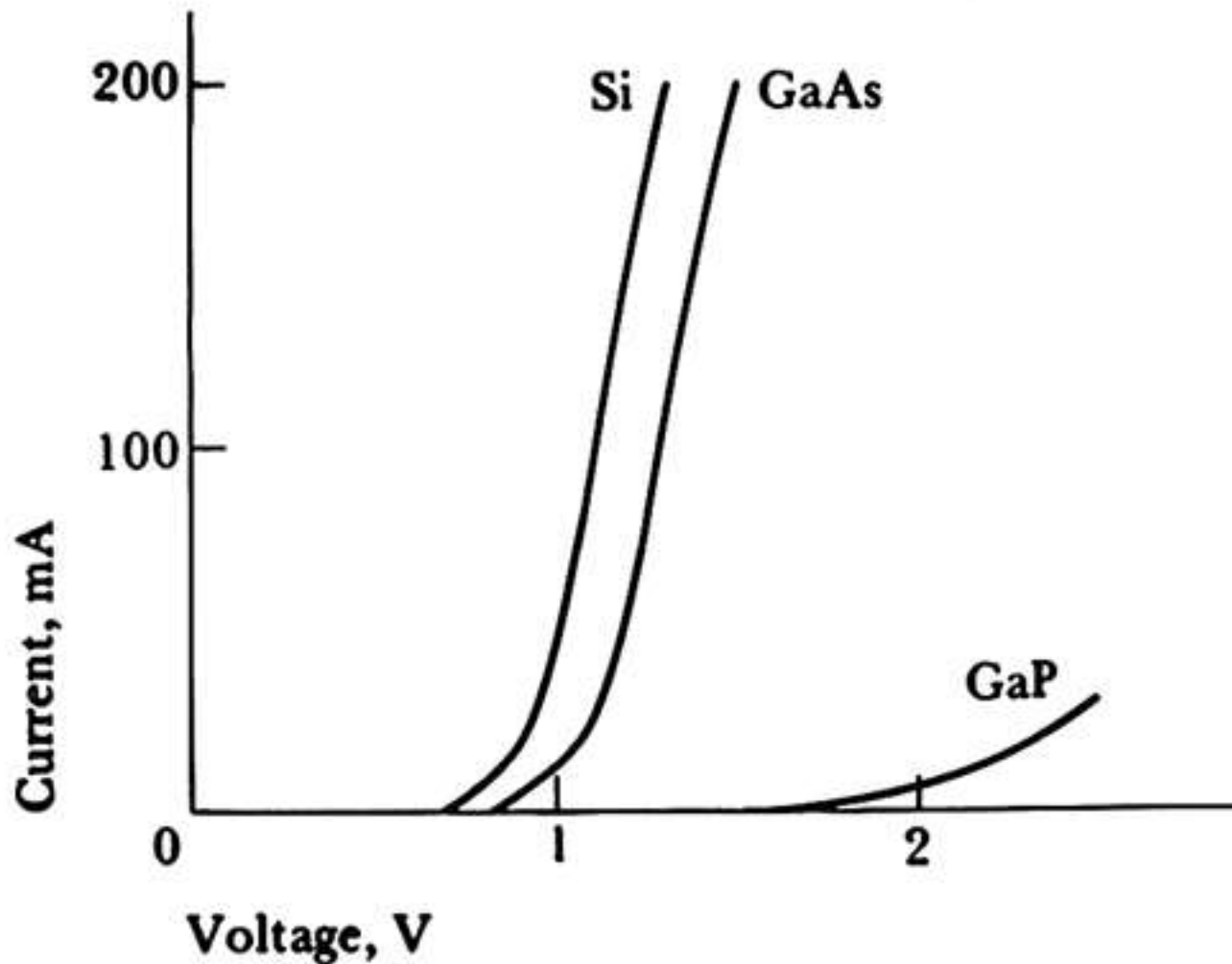


Figure 2.19 Forward characteristics for p-n junctions. Ordinary silicon diodes have a band gap of 1.1 eV and are inefficient radiators in the near-infrared. GaAs has a band gap of 1.44 eV and radiates at 900 nm. GaP has a band gap of 2.26 eV and radiates at 700 nm.

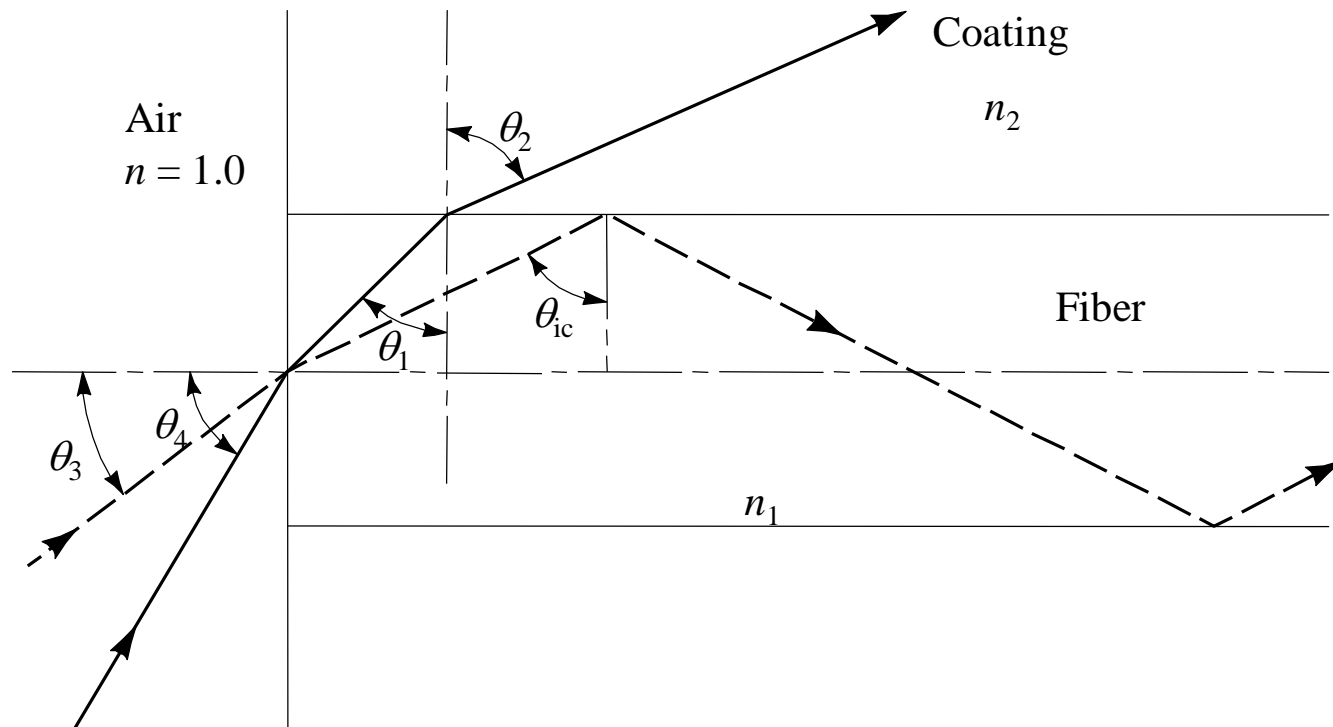


Figure 2.20 Fiber optics. The solid line shows refraction of rays that escape through the wall of the fiber. The dashed line shows total internal reflection within a fiber.

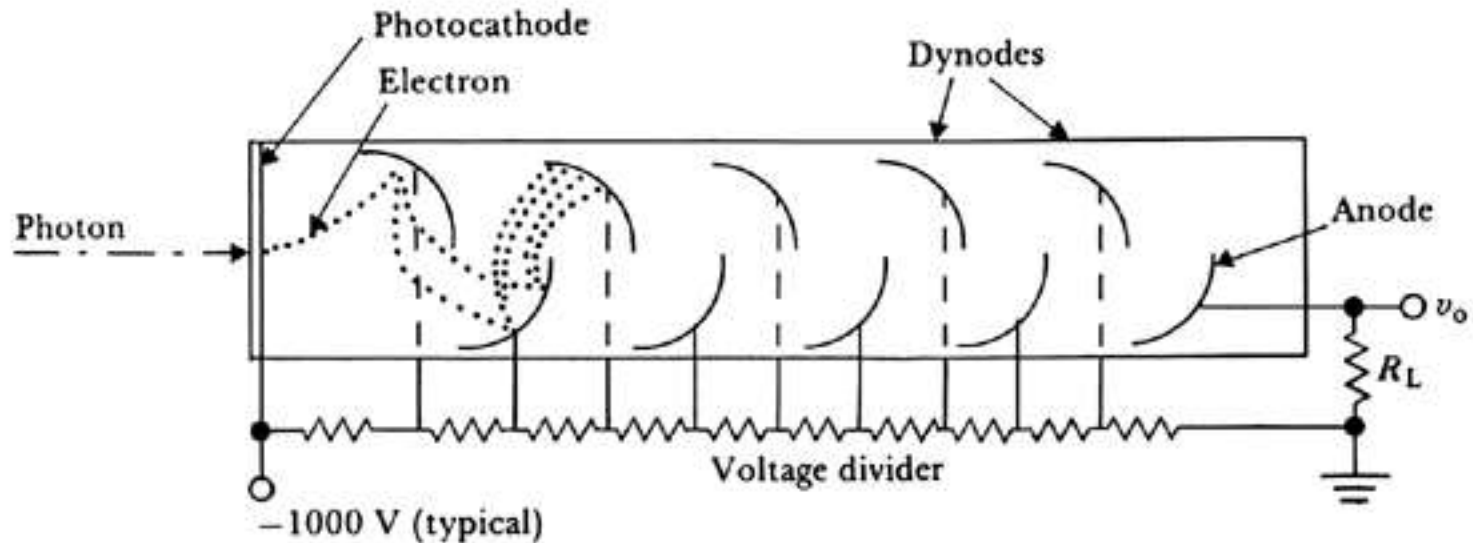


Figure 2.21 Photomultiplier An incoming photon strikes the photocathode and liberates an electron. This electron is accelerated toward the first dynode, which is 100 V more positive than the cathode. The impact liberates several electrons by secondary emission. They are accelerated toward the second dynode, which is 100 V more positive than the first dynode. This electron multiplication continues until it reaches the anode, where currents of about 1 μA flow through R_L .

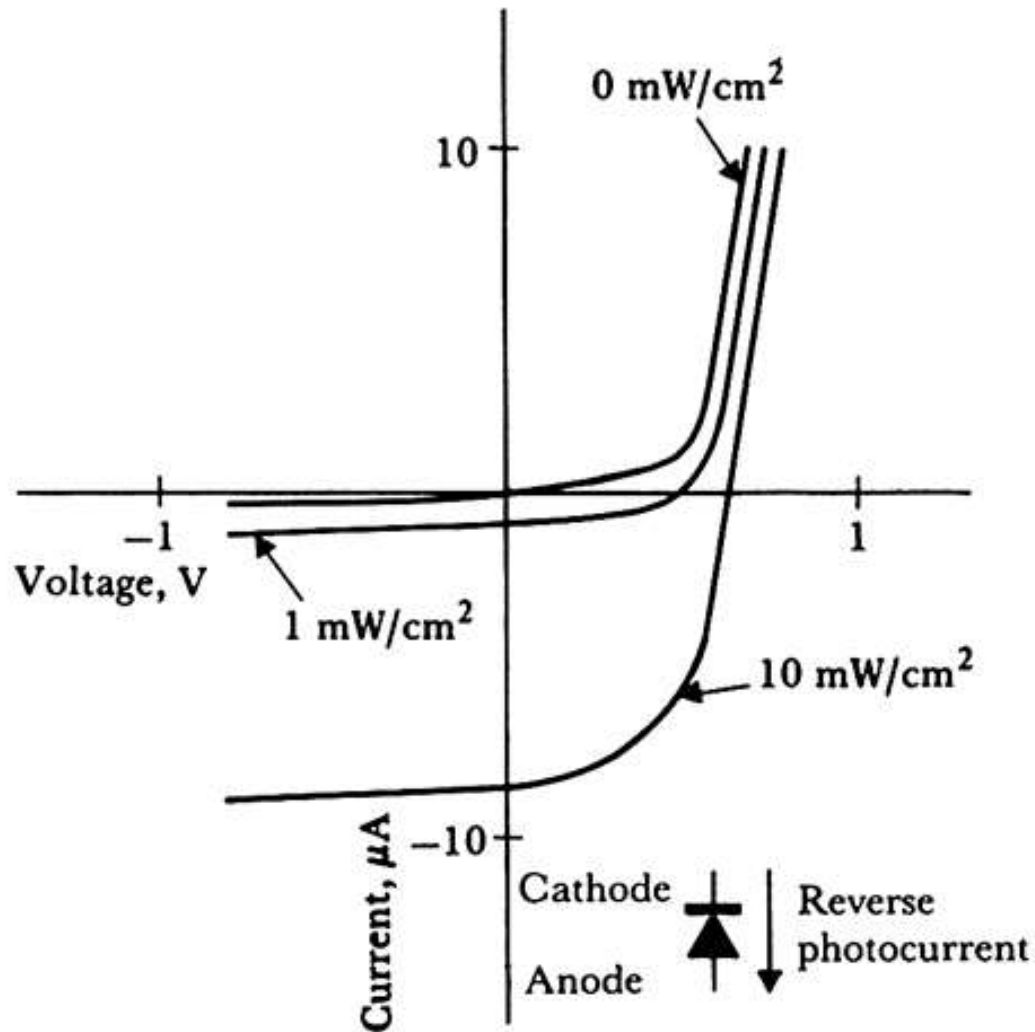


Figure 2.22 Voltage-current characteristics of irradiated silicon p-n junction. For 0 irradiance, both forward and reverse characteristics are normal. For 1 mW/cm², open-circuit voltage is 600 μV and short-circuit current is 8 μA.